Comparison of the magnetic properties of GeMn thin films through Mn L-edge x-ray absorption

S. Ahlers,[1] P. R. Stone,[2,3] N. Sircar,[1] E. Arenholz,[4] O. D. Dubon,[2,3] and D. Bougeard[1]

[1] *Walter Schottky Institut, Technische Universität München, Am Coulombwall 3, D-85748 Garching, Germany*

[2] *Department of Materials Science and Engineering, University of California, Berkeley, California 94720, USA*

[3] *Lawrence Berkeley National Laboratory, Berkeley, California 94720, USA*

[4] *Advanced Light Source, Lawrence Berkeley National Laboratory, Berkeley, California 94720, USA*

Abstract

X-ray absorption spectroscopy of epitaxial GeMn thin films reveals an experimentally indistinguishable electronic configuration of Mn atoms incorporated in $Ge_{1-x}Mn_x$ nanoclusters and in precipitates of the intermetallic compound Mn_5Ge_3, respectively. However, the average magnetic response of thin films containing $Ge_{1-x}Mn_x$ nanoclusters is lower than the response of films containing Mn_5Ge_3 precipitates. This reduced magnetic response of $Ge_{1-x}Mn_x$ nanoclusters is explained in terms of a fraction of Mn atoms being magnetically inactive due to antiferromagnetic coupling or the presence of structural disorder. A determination of the role of magnetically inactive Mn atoms in the self-assembly of the thermodynamically metastable $Ge_{1-x}Mn_x$ nanoclusters seems to be an essential ingredient for an enhanced control of this promising high Curie temperature magnetic semiconductor.

The material system Ge-Mn represents a promising candidate for magnetic semiconductor applications due to its compatibility to mainstream Si technology and the accessibility of Curie temperatures above room temperature.[1–3] The latter were observed in epitaxially fabricated GeMn thin films, where specific epitaxy conditions far from thermodynamic equilibrium lead to an inhomogeneous distribution of Mn in the Ge host in the form of self-assembled, nanometer-sized, Mn-rich regions coherently embedded in the Ge-rich host matrix.[1, 4] In addition to such thermodynamically metastable $Ge_{1-x}Mn_x$ nanoclusters, a small number of Mn_xGe_y intermetallic compounds are known, like for example Mn_5Ge_3. Mn_5Ge_3 is a magnetically hard compound[5] with a Curie temperature near room temperature[6] and a hexagonal lattice structure.[7] Proper control of the epitaxy conditions in the GeMn material system allows the deposition of layers containing only $Ge_{1-x}Mn_x$ nanoclusters, Mn_5Ge_3 precipitates or both,[8] which is of interest for composite magnetic semiconductor applications.

At present, the exact nature of the $Ge_{1-x}Mn_x$ nanoclusters and a microscopic explanation of the observed magnetism are unresolved issues. An atomic-scale investigation of these nanometer-sized regions embedded in a crystalline matrix by nanostructural imaging techniques such as transmission electron microscopy (TEM) is hampered by the difficulty to eliminate signals stemming from the embedding Ge matrix. Complementary information is expected from x-ray absorption (XA) spectroscopy, which is inherently element-selective and influenced by the local electronic structure and the charge state of the Mn impurities in the Ge matrix. Furthermore, by utilizing circularly-polarized photons we can examine the x-ray magnetic circular dichroism (XMCD) resulting from the presence of magnetically active Mn impurities.

In this letter, we compare samples with varying amounts of $Ge_{1-x}Mn_x$ nanoclusters and Mn_5Ge_3 precipitates through their XA and XMCD spectra at the Mn L-edge. We show that $Ge_{1-x}Mn_x$ nanoclusters exhibit a reduced average magnetic response compared to Mn_5Ge_3 precipitates in epitaxial thin films with equal total Mn content. In spite of these differences, XA spectroscopy (XAS) indicates a very similar local electronic and structural environment for Mn incorporated in $Ge_{1-x}Mn_x$ and intermetallic Mn_5Ge_3, respectively.

The thin films investigated in this work were fabricated by solid source low temperature molecular beam epitaxy on Ge(001) substrates. Details on the fabrication procedure are given in Ref. 8 and Ref. 4. All thin films were fabricated with a Ge flux rate of $r_{\mathrm{Ge}} =$

$0.08\,\text{Å}\,\text{s}^{-1}$ and a total Mn content of $x = 2.8\,\%$.

Structural properties were measured in cross-sectional TEM with an FEI Titan 80-300 microscope, magnetic properties in a commercial Quantum Design MPMS-XL superconducting quantum interference device (SQUID). Mn contents were measured by secondary ion mass spectroscopy using a Mn implanted standard. XA measurements at the Mn L-edge were carried out at the beamline 4.0.2[9] of the Advanced Light Source in the bulk sensitive[10] total fluorescence yield (TFY) mode. XMCD spectra, the difference in TFY for parallel and antiparallel alignment of an external magnetic field and photon helicity, were acquired in a magnetic field of 0.5 T applied collinear with the x-ray beam and at an angle of 30° to the sample surface. Prior to the measurement, the thin film surfaces were cleaned from Ge oxides by a deionized water dip.[11]

Three thin films, fabricated at substrate temperatures of $T_\mathrm{S} = 60\,°\mathrm{C}$, $85\,°\mathrm{C}$ and $120\,°\mathrm{C}$, are presented in this letter. The epitaxy was found to be controllable with the fabrication temperature. At $T_\mathrm{S} = 60\,°\mathrm{C}$, thin films consist solely of self-assembled Mn-rich $\mathrm{Ge}_{1-x}\mathrm{Mn}_x$ nanoclusters embedded in a Ge matrix with diamond-type lattice.[4] Increasing the fabrication temperature beyond $60\,°\mathrm{C}$ additionally leads to the precipitation of nanometer-sized inclusions of the intermetallic compound $\mathrm{Mn}_5\mathrm{Ge}_3$ in the Ge matrix.[8] This is shown in Fig. 1, where a cross-sectional TEM overview image of the $T_\mathrm{S} = 85\,°\mathrm{C}$ thin film is depicted. The image shows a dense assembly of nanometer-sized, elongated regions of dark contrast corresponding to self-assembled $\mathrm{Ge}_{1-x}\mathrm{Mn}_x$ nanoclusters. In addition several approximately round regions, indicated by the white dashed circles, are visible. These regions correspond to $\mathrm{Mn}_5\mathrm{Ge}_3$ precipitates with hexagonal $D8_8$ lattice structure.[7] In a higher magnification image these regions exhibit Moiré-patterns, which are due to a crystal structure differing from the surrounding Ge matrix with diamond-type lattice. Increasing the fabrication temperature further increases the amount of the $\mathrm{Mn}_5\mathrm{Ge}_3$ precipitates while the amount of self-assembled $\mathrm{Ge}_{1-x}\mathrm{Mn}_x$ nanoclusters decreases. At $T_\mathrm{S} = 120\,°\mathrm{C}$, only $\mathrm{Mn}_5\mathrm{Ge}_3$ precipitates are observed. In the temperature range $60\,°\mathrm{C} \leq T_\mathrm{S} \leq 120\,°\mathrm{C}$, the appearance of the thin films thus gradually changes from the exclusive presence of self-assembled $\mathrm{Ge}_{1-x}\mathrm{Mn}_x$ nanoclusters at $T_\mathrm{S} = 60\,°\mathrm{C}$ to a composite material containing both $\mathrm{Ge}_{1-x}\mathrm{Mn}_x$ nanoclusters and inclusions of intermetallic $\mathrm{Mn}_5\mathrm{Ge}_3$ at $T_\mathrm{S} = 85\,°\mathrm{C}$. Eventually, at $T_\mathrm{S} = 120\,°\mathrm{C}$, only $\mathrm{Mn}_5\mathrm{Ge}_3$ precipitates are present. Note that the total Mn content of the epitaxial film was not changed from film to film.

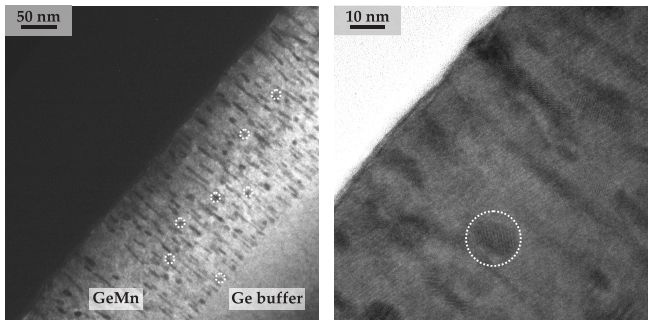

Figure 1: Cross-sectional TEM images. (left) Overview image and (right) close-up image. Dashed white circles mark regions exhibiting Moiré patterns.

XA spectra of the thin films acquired at the Mn $L_{3,2}$ edge are shown in Fig. 2(a) and (b). The absorption spectrum of the $T_S = 60\,°C$ $Ge_{1-x}Mn_x$ nanocluster thin film exhibits broad L_2 and L_3 peaks without a pronounced fine structure. XAS line shapes and $L_{3,2}$ absorption peak energies serve as a fingerprint for the electronic and structural configuration of the material under investigation. However, in spite of distinctively different crystal structure and chemical composition of $Ge_{1-x}Mn_x$ nanoclusters and Mn_5Ge_3 precipitates, [4, 8] the transition from solely $Ge_{1-x}Mn_x$ nanoclusters at $T_S = 60\,°C$ to solely Mn_5Ge_3 precipitates at $T_S = 120\,°C$ does not alter the XAS line shape nor results in a chemical shift of the $L_{3,2}$ energetic positions. All spectra resemble that of metallic Mn both in line shape and $L_{3,2}$ branching ratio, indicating the presence of metallic, delocalized $3d$ states of the absorbing Mn atoms in all thin films.[12–14]

The fact that the thin films exhibit a common XA fingerprint is further illustrated in Fig. 2(b), where the spectra of all thin films were scaled to match the L_3 peak intensity of the $T_S = 120\,°C$ thin film. Clearly, only the intensity of the spectra is decreased as the content in $Ge_{1-x}Mn_x$ nanoclusters is increased with decreasing T_S, demonstrated by the different scaling factors denoted in the figure.

The similarity in the XA fingerprints indicates a strong similarity in the electronic configuration of the Mn atoms incorporated in $Ge_{1-x}Mn_x$ nanoclusters and Mn_5Ge_3 precipitates, respectively. In particular charge state and – as far as the resulting spectral shape is not washed out due to the delocalized $3d$ electrons – also the local coordination of the absorbing Mn in $Ge_{1-x}Mn_x$ nanoclusters and Mn_5Ge_3 precipitates are indistinguishable within the resolution of the measurement.

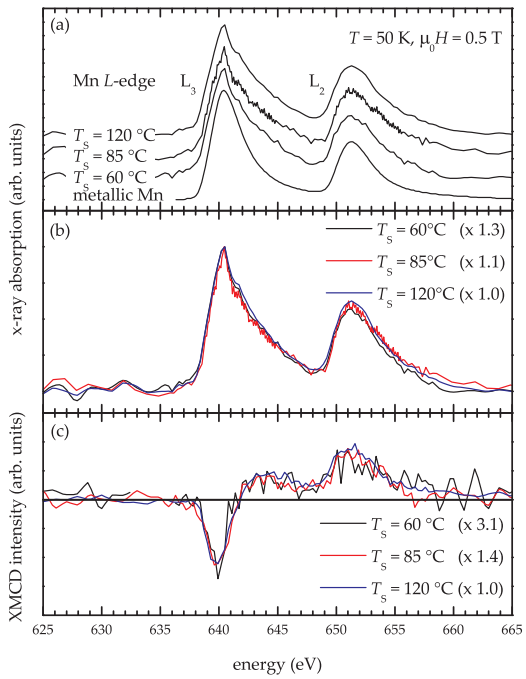

Figure 2: XA (a, b) and corresponding XMCD spectra (c) of thin films with increasing Mn_5Ge_3 content, measured at 50 K. Substrate temperatures are $T_S = 60\,°C$, $85\,°C$ and $120\,°C$, respectively. The total Mn content for all films is 2.8 %. For comparison, the absorption spectrum of metallic Mn is included in (a).[15] The XA and XMCD spectra are normalized to the L_3 peak intensity of the $T_S = 120\,°C$ thin film in (b) and (c), respectively. The scaling factors are given in the figures.

In order to investigate the magnetic activity of the incorporated Mn atoms, XMCD spectra were measured and are shown in Fig. 2(c). At $T_S = 60\,°C$, three broad peaks are observed in the XMCD spectrum. These three features are clearly distinguishable in spite of the small signal to noise ratio of the spectra. As in the case of the XA spectra, the XMCD spectra are indicative of metallic, delocalized Mn $3d$ states. Again, the transition from $Ge_{1-x}Mn_x$ nanoclusters to Mn_5Ge_3 precipitates does not alter the line shape of the XMCD spectra. However, the intensities of all three XMCD peaks decrease with increasing amount of $Ge_{1-x}Mn_x$ nanoclusters. The XMCD spectra shown in Fig. 2(c) are scaled to match the L_3 XMCD intensity of the $T_S = 120\,°C$ thin film and superimpose within the experimental error. The scaling factors are given in the figure. It is interesting to note that, according to the relative spin and orbital moment sum rules,[16] the scalability of the XMCD spectra translates into similar ratios of the spin and orbital moments of Mn incorporated in $Ge_{1-x}Mn_x$ nanoclusters and in Mn_5Ge_3 precipitates. Furthermore the scaling factors of

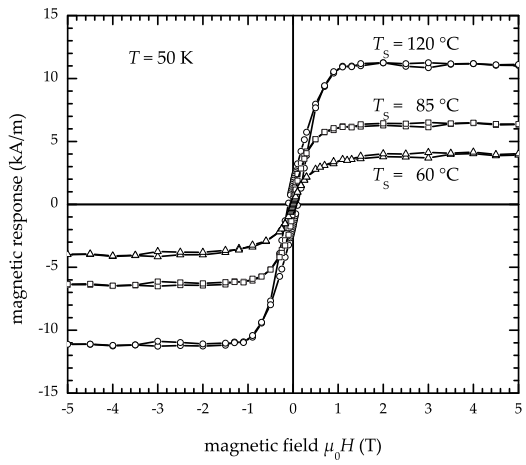

Figure 3: SQUID magnetization loops measured at 50 K. The total Mn content for all films is 2.8 %. Substrate temperatures are $T_S = 60\,°C$, $85\,°C$ and $120\,°C$.

the XAS and XMCD spectra infer a decreased average magnetic moment per Mn when $Ge_{1-x}Mn_x$ nanoclusters are introduced and their amount is increased at the expense of Mn_5Ge_3 precipitates.

This latter finding is corroborated by field dependent magnetization loops, recorded with conventional SQUID magnetometry and depicted in Fig. 3: In spite of an identical total Mn content in the three thin films, they display increasing magnetization with increasing fabrication temperature. The presence of $Ge_{1-x}Mn_x$ nanoclusters in the $T_S = 60\,°C$ and $T_S = 85\,°C$ thin films thus leads to reduced magnetic response compared to the $T_S = 120\,°C$ film containing only Mn_5Ge_3 precipitates. Since all samples contain the same total amount of Mn atoms, SQUID measurements also infer a reduced average magnetic moment per Mn atom when the amount of $Ge_{1-x}Mn_x$ nanoclusters is increased at the expense of Mn_5Ge_3 precipitates.

In our study XAS indicates an experimentally indistinguishable charge state and local coordination of Mn in all samples. XMCD underpins this similarity through an equal ratio of orbital and spin moment. At the same time, both XMCD as well as SQUID magnetometry measurements show that when increasing the amount of $Ge_{1-x}Mn_x$ nanoclusters at the expense of Mn_5Ge_3 precipitates, the magnetic response of the thin films decreases. These apparently opposing observations of a differing Mn magnetic moment with at the same time strong similarities in the Mn electronic environment and magnetic configuration leads to the conclusion that not every individual Mn atom contributes to the measured magnetic

response. Although being element-specific, XA like SQUID magnetometry delivers an information averaged over the total sample volume. We thus conclude that, while all Mn atoms exhibit similar atomic magnetic moments, a fraction of the atoms is magnetically inactive and therefore not contributing to the measured XMCD and SQUID magnetic response. The amount of the magnetically inactive Mn increases with the presence of nanoclusters and is highest in the absence of Mn_5Ge_3 precipitates at $T_S = 60\,°C$, hinting towards a relationship between the presence of nanoclusters and of a fraction of Mn atoms which do not contribute to the total magnetization.

Magnetic inactivity not only in $Ge_{1-x}Mn_x$, but also in other magnetic semiconductors may have various origins. These can be antiferromagnetic interaction between Mn atoms leading to magnetic frustration[17] and spin disorder.[18] They can also be Mn $3d$ states forming a low or zero moment, metallic impurity band as it was recently found in amorphous $Si_{1-x}Mn_x$.[15] The latter represents a noteworthy explanation for the magnetic inactivity observed in this work, since delocalized, metallic $3d$ states were indeed found in the XAS fingerprints presented in Fig. 2. Remarkably, hints for crystallographic disorder can be found in reports on epitaxially fabricated GeMn free of Mn_5Ge_3 precipitates.[1, 2, 19, 20] It will therefore be interesting to investigate the next-nearest neighbour coordination shells of the Mn atoms, for instance by extended XA fine structure analysis, in order to clarify the presence of such structural disorder and to ascertain to what extent disorder leads to the observed magnetic inactivity.

In summary, the combination of x-ray absorption spectroscopy, electron microscopy and magnetometry reveals a strong similarity of the Mn incorporation in $Ge_{1-x}Mn_x$ nanoclusters and in Mn_5Ge_3 precipitates. This close relationship suggests similar magnetic moments of the magnetically active Mn atoms contributing to the overall magnetization. The observed reduced average magnetic response of the thin films containing $Ge_{1-x}Mn_x$ nanoclusters is expected to be due to a certain fraction of magnetically inactive Mn atoms. Structural disorder stemming from $Ge_{1-x}Mn_x$ nanoclusters is considered as a noteworthy explanation for the observed magnetic inactivity. Investigating crystallographic disorder therefore appears to be an important and instructive task for further engineering of this promising magnetic semiconductor.

This work was funded by the German Science Foundation (DFG) via Schwerpunktprogramm SPP 1285 Halbleiter Spintronik and supported by the U.S. Department of Energy

under Contract No. DE-AC02-05CH11231. The authors acknowledge access to facilities of the Nanosystems Initiative Munich (NIM) and the Department of Chemistry, Technische Universität München, and support by M. Döblinger, T. F. Fässler, M. B. Boeddinghaus, R. Farshchi and S. Tardif. P.R.S. is furthermore grateful for support from NSF and NDSEG and D.B. for support by Alexander von Humboldt-Stiftung.

---

[1] M. Jamet, A. Barski, T. Devillers, V. Poydenot, R. Dujardin, P. Bayle-Guillemaud, J. Rothman, E. Bellet-Amalric, A. Marty, J. Cibert, R. Mattana, and S. Tatarenko, Nat. Mater. **5**, 653 (2006).

[2] A. P. Li, C. Zeng, K. van Benthem, M. F. Chisholm, J. Shen, S. V. S. N. Rao, S. K. Dixit, L. C. Feldman, A. G. Petukhov, M. Foygel, and H. H. Weitering, Phys. Rev. B **75**, 201201(R) (2007).

[3] C. Zeng, Z. Zhang, K. van Benthem, M. F. Chisholm, and H. H. Weitering, Phys. Rev. Lett. **100**, 066101 (2008).

[4] D. Bougeard, S. Ahlers, A. Trampert, N. Sircar, and G. Abstreiter, Phys. Rev. Lett. **97**, 237202 (2006).

[5] Y. Tawara and K. Sato, J. Phys. Soc. Jpn. **18**, 773 (1963).

[6] N. Yamada, J. Phys. Soc. Jpn. **59**, 273 (1990).

[7] J. B. Forsyth and P. J. Brown, J. Phys.: Condens. Matter **2**, 2713 (1990).

[8] S. Ahlers, D. Bougeard, N. Sircar, G. Abstreiter, A. Trampert, M. Opel, and R. Gross, Phys. Rev. B **74**, 214411 (2006).

[9] E. Arenholz and S. O. Prestemon, Rev. Sci. Instrum. **76**, 083908 (2005).

[10] Y. Idzerda, C. Chen, H.-J. Lin, G. Meigs, G. Ho, and C.-C. Kao, Nucl. Instrum. Methods Phys. Res. A **347**, 134 (1994).

[11] S. Rivillon, Y. J. Chabal, F. Amy, and A. Kahn, Appl. Phys. Lett. **87**, 253101 (2005).

[12] P. D. Padova, J. P. Ayoub, I. Berbezier, P. Perfetti, C. Quaresima, A. M. Testa, D. Fiorani, B. Olivieri, J. M. Mariot, A. Taleb-Ibrahimi, M. C. Richter, O. Heckmann, and K. Hricovini, Phys. Rev. B **77**, 045203 (2008).

[13] P. Gambardella, L. Claude, S. Rusponi, K. J. Franke, H. Brune, J. Raabe, F. Nolting, P. Bencok, A. T. Hanbicki, B. T. Jonker, C. Grazioli, M. Veronese, and C. Carbone, Phys. Rev. B

75, 125211 (2007).

[14] L. Sangaletti, D. Ghidoni, S. Pagliara, A. Goldoni, A. Morgante, L. Floreano, A. Cossaro, M. C. Mozzati, and C. B. Azzoni, Phys. Rev. B **72**, 035434 (2005).

[15] L. Zeng, A. Huegel, E. Helgren, F. Hellman, C. Piamonteze, and E. Arenholz, Appl. Phys. Lett. **92**, 142503 (2008).

[16] C. T. Chen, Y. U. Idzerda, H.-J. Lin, N. V. Smith, G. Meigs, E. Chaban, G. H. Ho, E. Pellegrin, and F. Sette, Phys. Rev. Lett. **75**, 152 (1995).

[17] K. W. Edmonds, N. R. S. Farley, T. K. Johal, G. van der Laan, R. P. Campion, B. L. Gallagher, and C. T. Foxon, Phys. Rev. B **71**, 064418 (2005).

[18] G. Zaránd and B. Jankó, Phys. Rev. Lett. **89**, 047201 (2002).

[19] M. Rovezzi, T. Devillers, E. Arras, F. d'Acapito, A. Barski, M. Jamet, and P. Pochet, Appl. Phys. Lett. **92**, 242510 (2008).

[20] S. Sugahara, K. Lee, S. Yada, and M. Tanaka, Jpn. J. Appl. Phys. **44**, L1426 (2005).

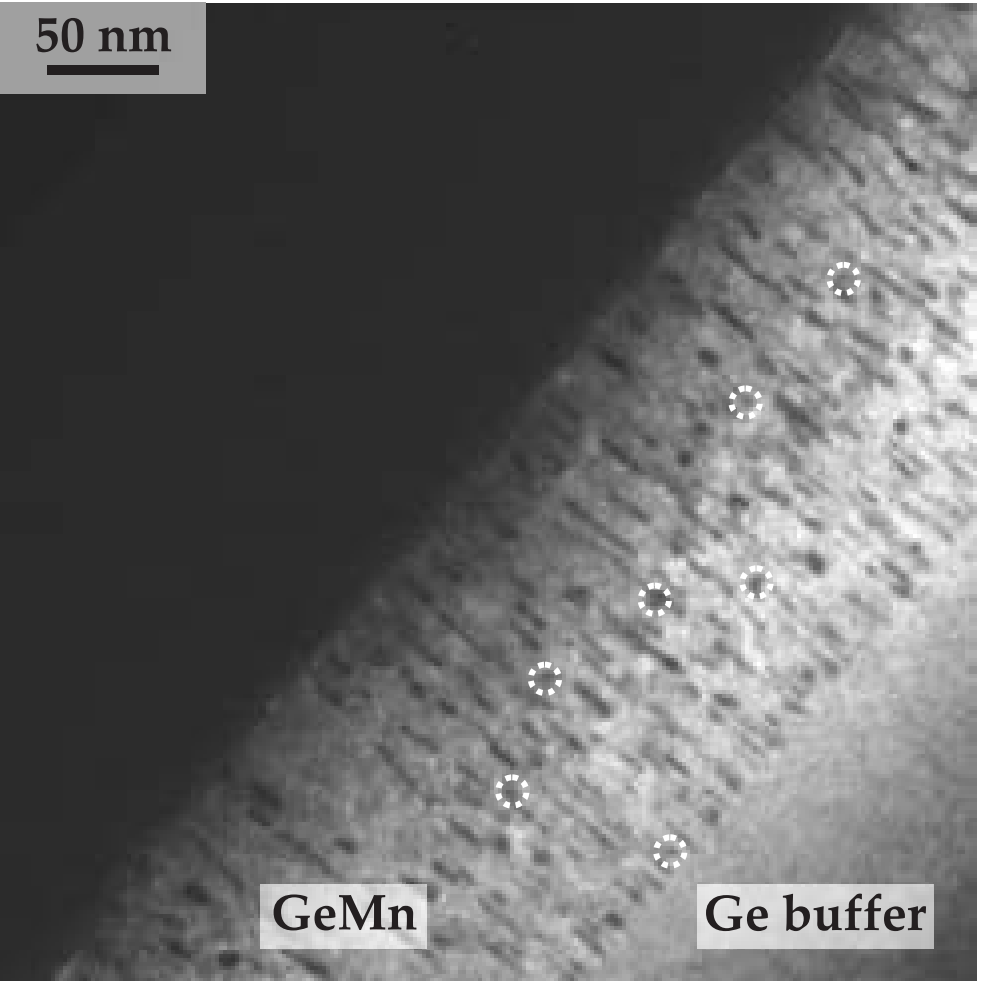
50 nm
GeMn
Ge buffer

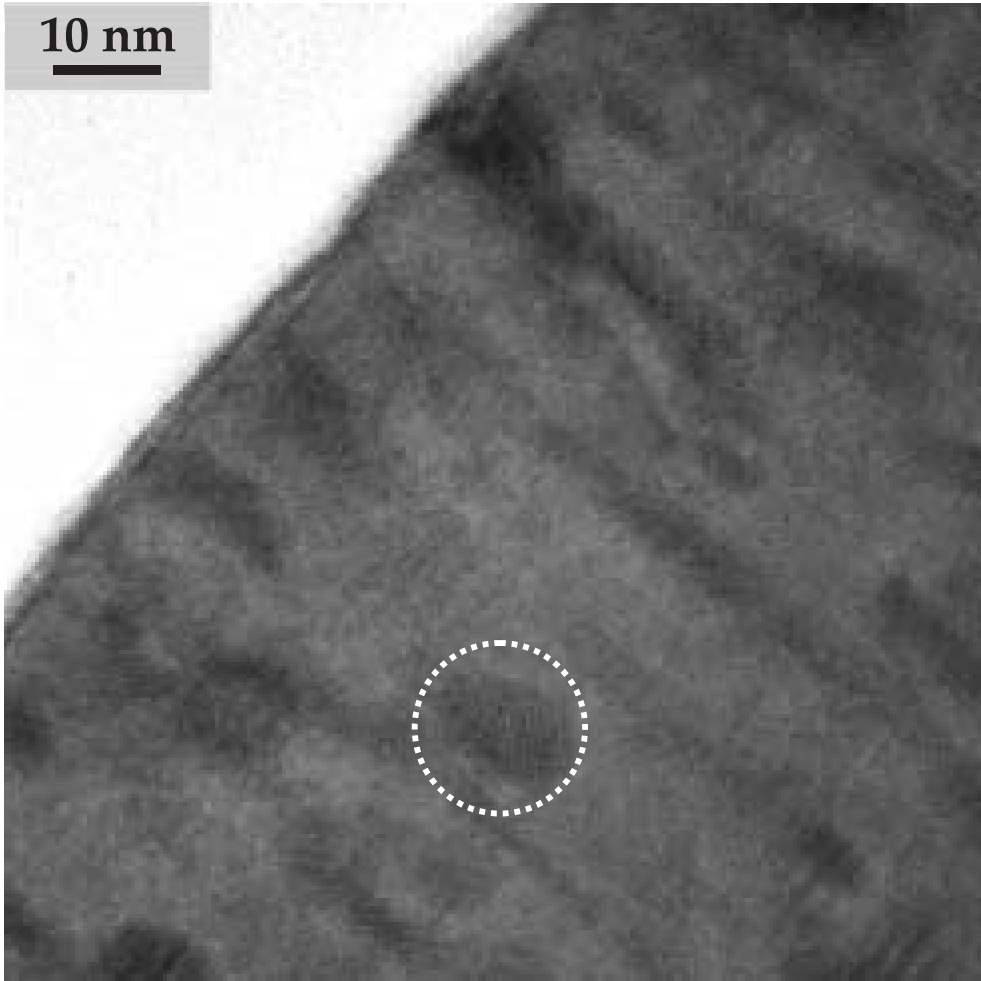
10 nm

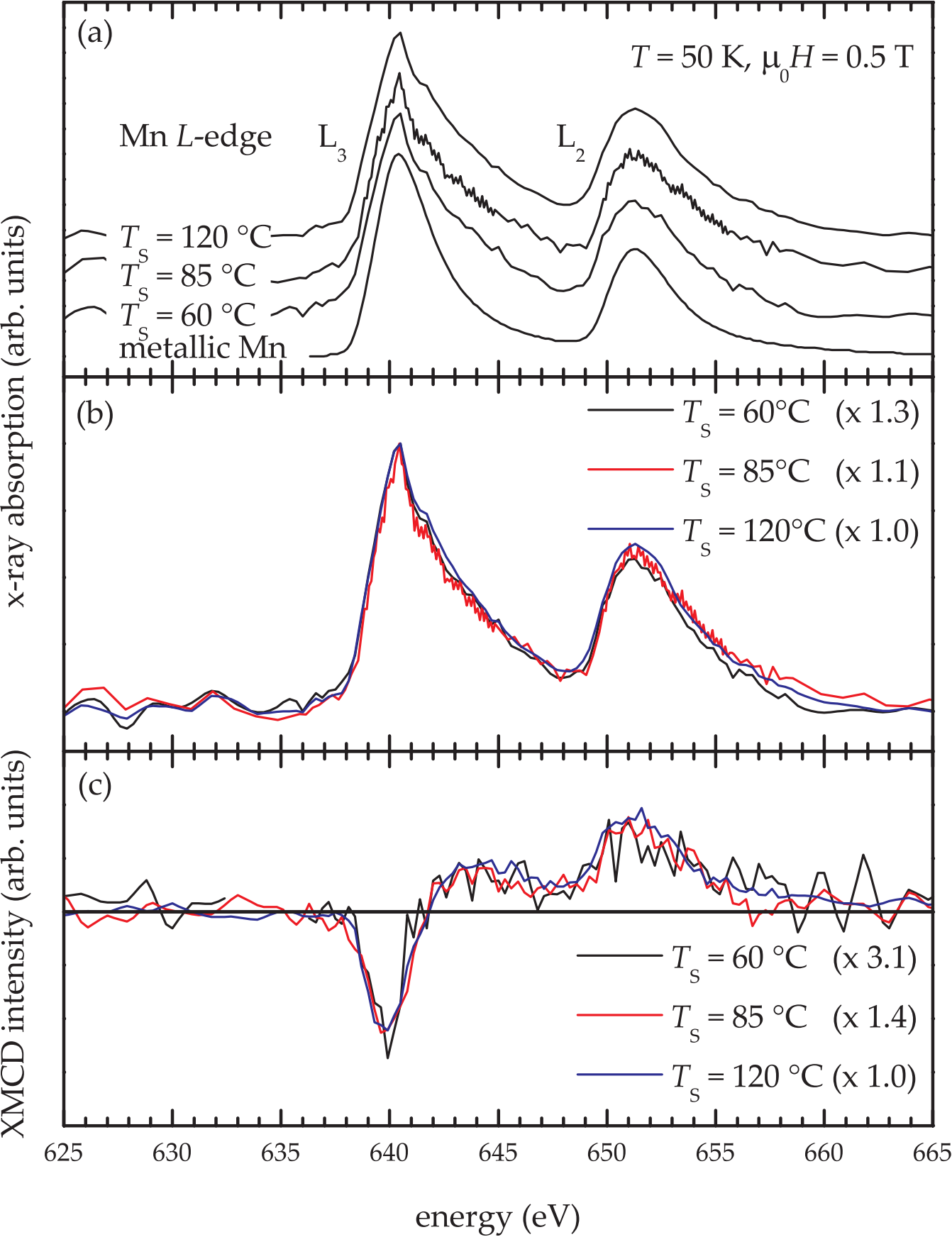
(a)
T = 50 K, μ0H = 0.5 T
Mn L-edge
L3
L2
Ts = 120 °C
Ts = 85 °C
Ts = 60 °C
metallic Mn
(b)
Ts = 60°C (x 1.3)
Ts = 85°C (x 1.1)
Ts = 120°C (x 1.0)
(c)
Ts = 60 °C (x 3.1)
Ts = 85 °C (x 1.4)
Ts = 120 °C (x 1.0)
x-ray absorption (arb. units)
XMCD intensity (arb. units)
625
630
635
640
645
650
655
660
665
energy (eV)

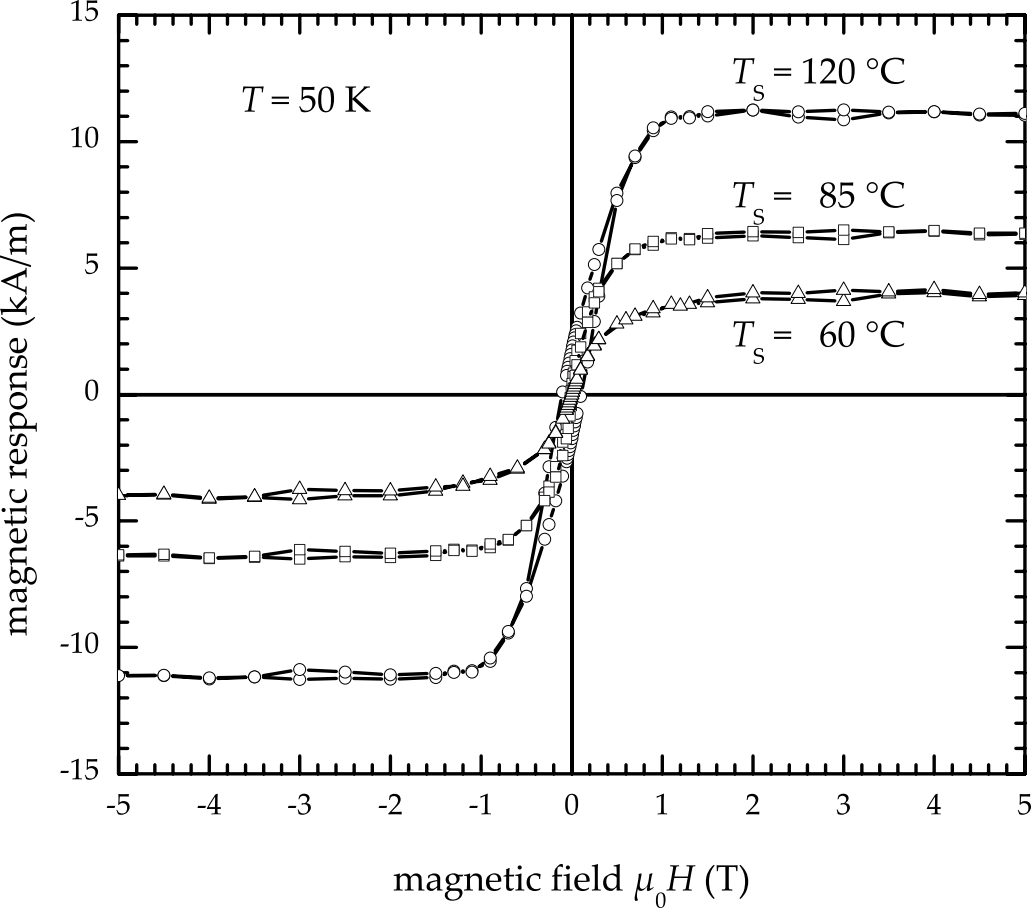
T = 50 K
T_S = 120 °C
T_S = 85 °C
T_S = 60 °C
magnetic response (kA/m)
magnetic field μ_0 H (T)
15
10
5
0
-5
-10
-15
-5
-4
-3
-2
-1
0
1
2
3
4
5